Journal of Experimental Botany, Vol. 65, No. 13, pp. 3759–3767, 2014
doi:10.1093/jxb/eru036 Advance Access publication 31 March, 2014

Journal of Experimental Botany
www.jxb.oxfordjournals.org

RESEARCH PAPER

Exploiting transplastomically modified Rubisco to rapidly measure natural diversity in its carbon isotope discrimination using tuneable diode laser spectroscopy

Susanne von Caemmerer*, Youshi Tazoe, John R. Evans and Spencer M. Whitney

Research School of Biology, The Australian National University, Canberra ACT 0200, Australia

* To whom correspondence should be addressed. E-mail: susanne.caemmerer@anu.edu.au

Received 26 September 2013; Revised 27 November 2013; Accepted 29 December 2013

Abstract

Carbon isotope discrimination (Δ) during C_3 photosynthesis is dominated by the fractionation occurring during CO_2-fixation by the enzyme Rubisco. While knowing the fractionation by enzymes is pivotal to fully understanding plant carbon metabolism, little is known about variation in the discrimination factor of Rubisco (*b*) as it is difficult to measure using existing *in vitro* methodologies. Tuneable diode laser absorption spectroscopy has improved the ability to make rapid measurements of Δ concurrently with photosynthetic gas exchange. This study used this technique to estimate *b in vivo* in five tobacco (*Nicotiana tabacum* L. cv Petit Havana [N,N]) genotypes expressing alternative Rubisco isoforms. For transplastomic tobacco producing *Rhodospirillum rubrum* Rubisco *b* was 23.8 ± 0.7‰, while Rubisco containing the large subunit Leu-335-Val mutation had a *b*-value of 13.9 ± 0.7‰. These values were significantly less than that for Rubisco from wild-type tobacco (*b*=29‰), a C_3 species. Transplastomic tobacco producing chimeric Rubisco comprising tobacco Rubisco small subunits and the catalytic large subunits from either the C_4 species *Flaveria bidentis* or the C_3-C_4 species *Flaveria floridana* had *b*-values of 27.8 ± 0.8 and 28.6 ± 0.6‰, respectively. These values were not significantly different from tobacco Rubisco.

Key words: C_4 photosynthesis, carbon isotope discrimination, *Flaveria*, Rubisco, tobacco, tuneable diode laser spectroscopy.

Introduction

Carbon isotope discrimination occurring during C_3 photosynthesis is determined by CO_2-diffusion processes from the atmosphere to the chloroplast and the biochemical fractionation occurring during CO_2 fixation by Rubisco and during respiratory and photorespiratory CO_2 release (Farquhar *et al.*, 1989a). The fact that Rubisco discriminates strongly against $^{13}CO_2$ is apparent in the isotopic signature of atmospheric CO_2 and this has become a tool for monitoring global CO_2 exchange processes (Mook *et al.*, 1983; Yakir and Sternberg, 2000). The strong $^{13}CO_2$ discrimination by Rubisco is the primary cause of depleted ^{13}C levels in plant biomass. This effect has proved experimentally versatile by allowing photosynthetic carbon isotope discrimination to be used as a tool to elucidate CO_2-diffusion processes through stomata and from the leaf intercellular airspace to the sites of Rubisco carboxylation in the chloroplast stroma of C_3 plant species (Evans *et al.*, 1986, 2009; Farquhar *et al.*, 1989b). Interpreting $^{13}CO_2$ discrimination in C_4 plants has proved more challenging as a CO_2-concentrating mechanism (CCM) operates that spatially localizes Rubisco in bundle sheath compartments with reduced access to atmospheric CO_2. In the C_4 photosynthetic CCM, initial fixation of atmospheric CO_2 occurs via phosphoenolpyruvate carboxylase (PEPC), which discriminates less against ^{13}C than Rubisco (Farquhar, 1983). C_4 acids diffuse into the bundle sheath where decarboxylation supplies CO_2 to Rubisco. As a result of this CCM pathway, photosynthetic carbon isotope discrimination is much less in C_4-plant species (Evans *et al.*, 1986; Henderson *et al.*, 1992).

The fractionation factor of Rubisco is difficult to measure and only a limited number of measurements exist (McNevin *et al.*, 2007 and references therein). Current methods rely on the purification of natural or recombinant Rubisco forms by processes that typically reduce catalytic activity (Sharwood *et al.*, 2008). In plants, algae, and cyanobacteria, Rubisco is a 520–550-kDa L_8S_8 hexadecamer composed of eight ~50-kDa catalytic large (L) subunits and eight ~12–15-kDa small (S) subunits (Whitney *et al.*, 2011a). In most applications of photosynthetic carbon isotope discrimination, the fractionation factor of plant L_8S_8 Rubisco is assumed to be ~29‰, a value reproducibly derived for spinach Rubisco *in vitro* using a range of experimentally complex methodologies (Roeske and O'Leary, 1984) and supported by *in vivo* measurements of carbon isotope discrimination in transgenic tobacco with reduced amounts of Rubisco (Evans *et al.*, 1994). However, the evolutionary diversity in Rubisco catalysis (Yeoh *et al.*, 1981; Badger and Andrews, 1987; Tcherkez *et al.*, 2006), even among closely related C_3 species (Delgado *et al.*, 1995; Galmes *et al.*, 2005), brings into question the validity of this assumption. This catalytic diversity may conceivably arise from subtle variations to the reaction mechanism of Rubisco. Differences in the fractionation factor of Rubisco pose a useful means for interpreting such reaction mechanism variations (Tcherkez *et al.*, 2006; McNevin *et al.*, 2007; Tcherkez, 2013).

Transgenic tobaccos with altered amounts or forms of Rubisco have been used to quantify the enzyme's kinetic properties using leaf gas exchange and photosynthesis models. This *in vivo* approach has been particularly successful in determining the Michaelis–Menten constants for CO_2 and O_2 (K_c and K_o), catalytic turnover rates (V_{Cmax} and V_{Omax}) and CO_2/O_2 specificity of tobacco Rubisco and how they vary with temperature (von Caemmerer *et al.*, 1994; Bernacchi *et al.*, 2002; Walker *et al.*, 2013). The approach has also been successfully applied to catalytically altered Rubisco isoforms expressed in tobacco using chloroplast transformation technology (Whitney *et al.*, 1999; Whitney and Andrews, 2003; Sharwood *et al.*, 2008). More recent developments in tuneable diode laser (TDL) absorption spectroscopy have improved the ability to make rapid measurements of carbon isotope discrimination concurrently with photosynthetic gas exchange (Tazoe *et al.*, 2011). The current study combines this technique with transplastomic tobacco lines expressing alternative Rubisco isoforms to measure the Rubisco discrimination factor *in vivo*. The results confirm the fractionation factors determined *in vitro* for Rubisco from *Rhodospirillum rubrum* and the mutant tobacco Leu-335-Val (L335V) Rubisco (McNevin *et al.*, 2007) and also show that Rubisco fractionation factors for Rubisco from *Flaveria bidentis* (a C_4 species) and *Flaveria floridana* (C_3-C_4 intermediate species) are similar to that from tobacco (a C_3 species).

Materials and methods

Plant material

This study used wild-type tobacco (tob(Wt), *Nicotiana tabacum* L. cv Petit Havana [N,N]) and transplastomic mutants producing *R. rubrum* Rubisco (tob(Rr), Whitney and Andrews, 2001), mutant tobacco Rubisco containing the large subunit Leu-335-Val substitution (tob(L335V), Whitney *et al.*, 1999), or hybrid Rubisco comprising tobacco small subunits and *F. bidentis* (tob(bid), Whitney *et al.*, 2011b) or *F. floridana* (tob(flo), Whitney *et al.*, 2011b) large subunits. As some of the transplastomic mutants could not grow in air, all plants were grown in a growth chamber supplemented with 1% (v/v) CO_2. The air temperature was 25 °C with a 14-h photoperiod (400 µmol photon m^{-2} s^{-1}) and 60% relative humidity.

Concurrent gas exchange and carbon isotope discrimination measurements

Gas exchange and carbon isotope discrimination measurements were made as described by Tazoe *et al.* (2011) using either a 6-cm^2 chamber of the LI-6400 with a red-blue light-emitting diode (LED) light source (Li-Cor, Lincoln, Nebraska, USA) or a laboratory-constructed whole-leaf chamber (115 × 110 × 25 mm depth, boundary layer conductance 4 mol m^{-2} s^{-1}) together with a red-green-blue LED light source (6400–18 RGB Light source, Li-Cor) and the LI-6400. The flow rate was set at 200 µmol s^{-1}. Gas exchange was coupled to a tuneable diode laser (TDL, TGA100, Campbell Scientific, Logan, UT, USA) for concurrent measurements of carbon isotope composition. Measurements were made at 4-min intervals for 20 s and between six and eight measurements were made at each CO_2 partial pressure at an irradiance of 1500 µmol quanta m^{-2} s^{-1}. Other measurement conditions were O_2 19 mbar, and a leaf temperature 25 ºC. The LI-6400 CO_2 mixing system was used to generate different CO_2 concentrations. The $\delta^{13}C$ of CO_2 gas cylinders ($\delta^{13}C_{\mathrm{tank}}$) used in the LI-6400 CO_2 injector system was between –13 and –3‰. Gas exchange was calculated using the equations presented by von Caemmerer and Farquhar (1981) and Δ was calculated from the equation presented by Evans *et al.* (1986) as:

$$\Delta = \frac{1000\xi\left(\delta^{13}C_{sam} - \delta^{13}C_{ref}\right)}{1000 + \delta^{13}C_{sam} - \xi\left(\delta^{13}C_{sam} - \delta^{13}C_{ref}\right)} \quad (1)$$

where $\delta^{13}C_{\mathrm{sam}}$ and $\delta^{13}C_{\mathrm{ref}}$ are the carbon isotope compositions of the leaf chamber and reference air of the LI-6400, respectively, ξ is $C_{\mathrm{ref}}/(C_{\mathrm{ref}}-C_{\mathrm{sam}})$, where C_{ref} and C_{sam} are the CO_2 concentrations of dry air entering and exiting the leaf chamber, respectively, measured by the TDL. The value of ξ ranged from 4.5 to 13 for tob(Wt), 15 to 25 for tob(L335V), 15 to 16 for tob(Rr), 11 to 16 for tob(bid), and 8 to 15 for tob(flor).

Biochemical measurements

Following gas exchange, replicate leaf samples (0.5 cm^2) were taken from the sampling area and immediately frozen in liquid nitrogen and stored at –80 °C. Rubisco content in each sample was measured by the [^{14}C]carboxyarabinitol–P_2-binding assay procedure according to Ruuska *et al.* (1998). Soluble leaf protein was measured relative to BSA with a dye-binding assay (Pierce Coomassie Plus Kit). Dry mass of leaves were measured after 48 h at 80 °C. Leaf dry mass per unit area was calculated from destructive harvest data taken from 10 plants after 34 d.

Rubisco kinetic properties of Rubisco in tob(Rr) leaf protein extract was measured at 25 °C using $^{14}CO_2$-fixation assays as described (Whitney and Sharwood, 2007; Sharwood *et al.*, 2008). Assays were performed in 8-ml septum capped vials containing 1 ml reaction buffer [50 mM HEPES-NaOH pH 7.8, 15 mM $MgCl_2$, 0.25 mM ribulose bisphosphate (RuBP)] and varying concentrations of $NaH^{14}CO_3$ (9–952 µM) and O_2 (0, 10, 15 and 20% (v/v), accurately mixed with nitrogen using Wosthoff gas mixing pumps). Leaf protein was extracted in activation buffer [50 mM HEPES-NaOH pH 7.8, 15 mM $MgCl_2$, 20 mM $NaH^{14}CO_3$, 0.5 mM EDTA, 2 mM dithiothreitol, 1%, v/v, plant protease inhibitor cocktail (Sigma-Aldrich), and 1%, w/v, polyvinylpolypyrrolidone] and the Rubisco was activated at 25 °C for 10 min prior to using 20 µl to initiate the assays. The Michaelis constants (K_m) for CO_2 (K_c) and O_2 (K_o) were determined from the fitted data. The maximal carboxylation rate extrapolated from Michaelis–Menten curve fitting was divided by the amount of Rubisco active sites quantified by [^{14}C]carboxyarabinitol-P_2 binding (Ruuska *et al.*, 1998; Whitney and Andrews, 2001) to give k_{ccat}.

Calculation of Rubisco fractionation and mesophyll conductance

A full description of discrimination during C_3 photosynthesis is given by Evans *et al.* (1986). However, Farquhar and Cernusak (2012) pointed out that while equations used to calculate gas exchange include ternary effects of transpiration rate on the rate of CO_2 assimilation through stomata (von Caemmerer and Farquhar, 1981), the equations describing carbon isotope discrimination had been derived without the ternary effects. They introduced revised equations, and these are used in the current calculation:

$$\Delta = \frac{1}{1-t}a' + \frac{1}{1-t}\left((1+t)b - a'\right)\frac{C_i}{C_a} - \frac{1+t}{1-t}\left(b - a_i - \frac{eR_d}{(A+R_d)}\right)\frac{A}{g_m C_a} - \frac{1+t}{1-t}\left(\frac{eR_d}{(A+R_d)C_a}(C_i - \Gamma_*)\right) - \frac{1+t}{1-t}\left(f\frac{\Gamma_*}{C_a}\right) \quad (2)$$

where

$$t = \frac{(1+a')E}{2g_{ac}^{t}}$$

E denotes the transpiration rate, and g_{ac}^{t} denotes the total conductance to CO_2 diffusion including boundary layer and stomatal conductance (von Caemmerer and Farquhar, 1981). C_a and C_i are the ambient and intercellular CO_2 partial pressures and Γ_* is the compensation point in the absence of mitochondrial respiration. A and R_d stand for CO_2-assimilation rate and mitochondrial respiration in the light.

The mesophyll conductance to CO_2 diffusion from intercellular airspace to the chloroplast, g_m, is given by:

$$g_m = A/(C_i - C_c) \quad (3)$$

where C_c is the CO_2 partial pressure in the chloroplast. The symbol a_i (1.8‰) denotes the fractionation factor for hydration and diffusion through water, and b (usually ~29‰) is the fractionation associated with Rubisco carboxylation. The symbol a' denotes the combined fractionation factor through the leaf boundary layer and through stomata:

$$a' = \frac{a_b(C_a - C_s) + a(C_s - C_i)}{(C_a - C_i)} \quad (4)$$

where C_s is the CO_2 partial pressure at the leaf surface, a_b (2.9‰) is the fractionation occurring through diffusion in the boundary layer and a (4.4‰) is the fractionation due to diffusion in air (Evans *et al.*, 1986). The current study uses the photorespiratory fractionation factor f (16.2‰), determined by Evans and von Caemmerer (2013). Following Tazoe *et al.* (2009), no fractionation by day respiration is assumed and e is calculated as $\delta^{13}C_{tank}$–$\delta^{13}C_{atmosphere}$ (Wingate *et al.* 2007). In this study, $\delta^{13}C_{tank}$ ranged from –13.3 to –3‰ and $\delta^{13}C_{atmosphere}$ was –18‰ for plants grown in a growth cabinet with CO_2 enrichment (McNevin *et al.*, 2007).

Evans and von Caemmerer (2013) solved equation 2 for g_m, but this study has solved it for the Rubisco fractionation factor b:

$$b = \frac{\Delta - \frac{a'}{1-t}\left(1 - \frac{C_i}{C_a}\right) + \Delta_e + \Delta_f - \frac{1+t}{1-t}\left[\left(a_i + \frac{eR_d}{A+R_d}\right)\frac{A}{g_m C_a}\right]}{\frac{1+t}{1-t}\left(\frac{C_i}{C_a} - \frac{A}{g_m C_a}\right)} \quad (5)$$

where

$$\Delta_e = \frac{1+t}{1-t}\left(\frac{eR_d}{(A+R_d)C_a}(C_i - \Gamma_*)\right) \quad (6)$$

is most of the fractionation associated with respiration and

$$\Delta_f = \frac{1+t}{1-t}\left(f\frac{\Gamma_*}{C_a}\right) \quad (7)$$

is the fractionation associated with photorespiration.

Results

Gas exchange and biochemical properties of tobacco genotypes

This study used five tobacco (*N. tabacum* L. cv Petit Havana [N,N]) genotypes: wild-type [tob(Wt)] and transplastomic mutants producing homodimeric L_2 *R. rubrum* Rubisco [tob(Rr)], Whitney and Andrews, 2001; tobacco Rubisco containing the L-subunit Leu-335-Val mutation [tob(L335V)], Whitney *et al.*, 1999, or producing chimeric L_8S_8 Rubisco comprising tobacco S-subunits and either the *F. bidentis* L-subunit [tob(bid)], Whitney *et al.*, 2011b or the *F. floridana* L-subunit [tob(flo)], Whitney *et al.*, 2011b]. Table 1 summarizes *in vitro* catalytic properties of these enzymes and compares them to the catalytic properties of the native enzyme.

All gas exchange measurements were made at low O_2 partial pressure (19 mbar, ~2% atmospheric pO_2) to ensure adequate CO_2-assimilation rates could be measured at intercellular CO_2 pressures between 100 and 800 μbar for all tobacco genotypes and to minimize photorespiratory fractionation. CO_2 response curves of tob(Wt) show a clear transition from a Rubisco-limited to an RuBP-regeneration-limited response, whereas the other four genotypes remain Rubisco limited over the measured range in intercellular pCO_2, with lower CO_2-assimilation rates compared to wild type (Fig. 1). In tob(bid) and tob(flo) leaves, reduced CO_2-assimilation rates were associated with a 2.5–4-fold lower Rubisco content in their leaves compared to wild type (Table 2 and Fig. 1A). Conversely, both tob(Rr) and tob(L335V) had slightly more Rubisco than wild type on a leaf area basis (Table 2), but the combination of lower $S_{c/o}$ and reduced carboxylation efficiencies (K_{ccat}/K_c) resulted in CO_2-assimilation rates that were still carboxylation limited at 800 μbar pCO_2 and 19 mbar pO_2 (Fig. 1B). Even under these low O_2 conditions, both tob(L335V) and tob(Rr) have higher CO_2 compensation points compared with tob(Wt), consistent with their significantly lower Rubisco CO_2/O_2 specificity ($S_{c/o}$) and lower K_{ccat}/K_c ratios (Table 1 and Fig. 1B). Although Rubisco from tob(bid) and tob(flo) share comparable $S_{c/o}$ values with tob(Wt) (Table 1), their lower K_{ccat}/K_c ratios increase their compensation points (Fig. 1A).

Maximum Rubisco activity, V_{cmax}, was estimated from CO_2 response curves using the photosynthetic model of Farquhar et al. (1980). *In vitro* Rubisco kinetic constants K_c, K_o, and $S_{c/o}$ given in Table 1 were used, with

Table 1. *In vitro Rubisco kinetic constants of wild-type tobacco and* Flaveria floridana*,* Flaveria bidentis*,* Rhodospirillum rubrum*, and transplastomic mutants tob(flo), tob(bid), tob(Rr), and tob(L335V)*

To convert values from concentrations to partial pressures, solubilities for CO_2 of 0.0334 mol (l bar)$^{-1}$ and for O_2 of 0.00126 mol (l bar)$^{-1}$ were used. Atmospheric pressure in Canberra has an average of 953 mbar.

Rubisco type	$S_{c/o}$ (MM^{-1})	$S_{c/o}$ (bar bar^{-1})	k_{ccat} (s^{-1})	K_c (μM)	K_c (μbar)	k_{ocat} (s^{-1})	K_o (μM)	K_o (mbar)	Reference
Tobacco	81 ± 1	2147 ± 27	3.2 ± 0.2	12.6 ± 0.2	377 ± 6	0.8	274 ± 18	217 ± 14	Whitney *et al.* (2011)
F. floridana	82 ± 2	2174 ± 53	3.6 ± 0.1	14.4 ± 0.5	431 ± 15	1.1	374 ± 33	297 ± 26	
tob(flo)	81 ± 2	2147 ± 53	3.7 ± 0.2	14.5 ± 0.3	434 ± 9	1.2	359 ± 22	285 ± 17	
F. bidentis	81 ± 1	2147 ± 27	4.8 ± 0.3	20.4 ± 0.5	611 ± 15	1.2	420 ± 37	333 ± 29	
tob(bid)	79 ± 2	2094 ± 53	4.7 ± 0.2	19.9 ± 0.6	596 ± 18	1.2	408 ± 28	324 ± 22	
R. rubrum	9 ± 0.3	239 ± 8	12.3 ± 0.3	149 ± 8	4461 ± 240	1.4	159 ± 25	126 ± 19	Mueller-Cajar *et al.* (2007)
tob(Rr)	12 ± 1	318 ± 27	5.4 ± 0.3	96 ± 5	2874 ± 150	0.34	72 ± 9	57 ± 7	This study
tob(L335V)	20 ± 2	530 ± 53	0.8 ± 0.1	5.1 ± 0.8	153 ± 24	0.4	49 ± 11	38.9 ± 8.7	Whitney *et al.* (1999)

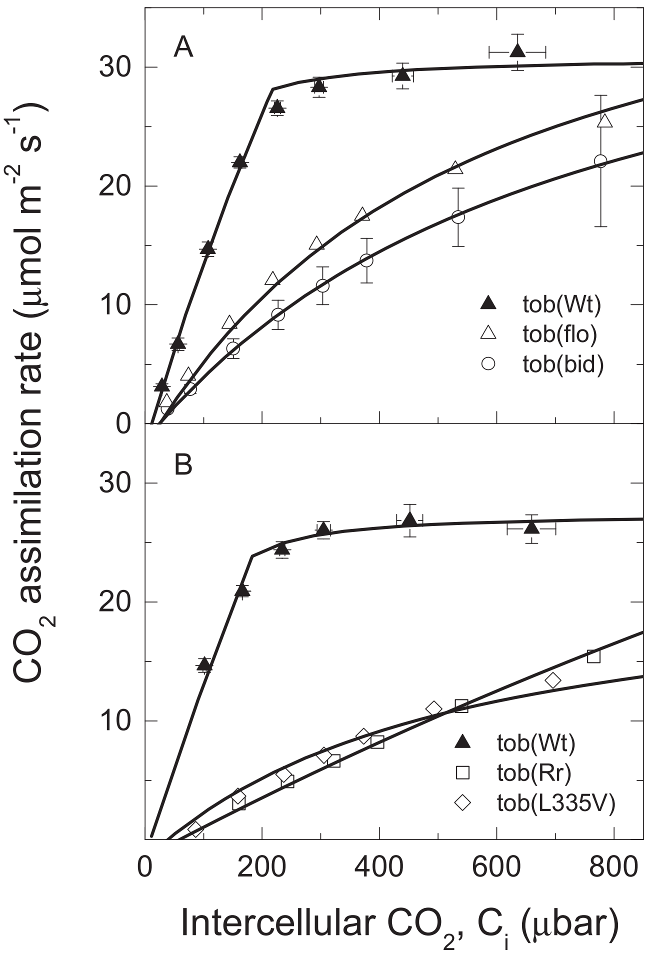

Fig. 1. (A) CO_2-assimilation rate, *A*, as a function of intercellular CO_2 partial pressure in tobacco wild type [tob(wt)] and two transplastomic mutants producing large subunits of *Flaveria bidentis* [tob(bid)] or *F. floridana* [tob(flo)]. Measurements were made on four tob(wt), three tob(bid), and three tob(flo) replicate plants and bars show standard errors. (B) CO_2-assimilation rate, *A*, as a function of intercellular CO_2 partial pressure in tob(Wt) and two transplastomic mutants producing *R. rubrum* Rubisco [tob(Rr)] or tobacco mutant Rubisco [tob(L335V)]. Measurements were made on four tob(Wt), four tob(Rr), and seven tob(L335V) replicate plants and bars show standard errors. Gas exchange measurements were made at various CO_2 partial pressures, O_2 19 mbar, irradiance 1500 μmol m^{-2} s^{-1}, and leaf temperature 25 °C. Model curves have been fitted to each genotype with the following values from Tables 1 and 2 [except tob(L335V); see text] and for K_c (μbar), K_o (mbar), Γ_* (μbar), R_d (μmol m^{-2} s^{-1}) and V_{cmax} (μmol m^{-2} s^{-1}). In A, for tob(Wt) 377, 217, 4.66, 1.8, 111.8, for tob(flo) 434, 285, 46.6, 1.9, 46.6, for tob(bid) 596, 324, 4.78, 1.3, 43.4, using g_m 0.46 mol m^{-2} s^{-1} bar^{-1}, and *J* 130.8 μmol m^{-2} s^{-1}. In B, for tob(Wt) 377, 217, 4.66, 1.4,134.3, for tob(Rr) 2874, 57, 31.44, 0.8, 112.4, for tob(L335V) [in vivo constants used, see text] 318, 55.6, 140, 1.24, 23.4, using g_m 0.29 mol m^{-2} s^{-1} bar^{-1}, and *J* 115.6 μmol m^{-2} s^{-1}.

the exception of tob(L335V) where *in vivo* constants from Whitney *et al.* (1999) were used. CO_2 partial pressures at the sites of carboxylation were calculated using the mesophyll conductance derived from wild-type tobacco grown at the same time (Table 2). Estimates of *in vivo* k_{ccat}, calculated by dividing V_{cmax} by Rubisco site content per unit leaf area, assuming full activation, reflected *in vitro* variation in Table 1.

Stomatal conductance was relatively unchanged for the four tobacco mutants, despite having lower CO_2-assimilation rates. Consequently, the mutants had greater ratios of intercellular to ambient CO_2 (C_i/C_a; Table 2) for most of the pCO_2 conditions tested (Fig. 2).

Carbon isotope discrimination of tobacco genotypes

This study measured the carbon isotope discrimination (Δ, ‰) concurrently with gas exchange using tuneable laser spectroscopy (Figs 2 and 3). The discrimination by both tob(bid) and tob(flo) was greater than that of tob(Wt) at all pCO_2 (Fig. 2A). Under the range of pCO_2 examined, carbon isotope discrimination by tob(L335V) was considerably less than tob(Wt) (Fig. 2B). In contrast, tob(Rr) had a greater discrimination at low pCO_2 and became more similar to tob(Wt) at high pCO_2. Discrimination is also shown against C_i/C_a (Fig. 3) because discrimination is strongly influenced by C_i/C_a. C_i/C_a was greater for all the mutants compared to tob(Wt) with the exception of tob(L335V) at high pCO_2 (Fig. 2 C and D).

The average values of carbon isotope discrimination at ambient pCO_2 are shown in Table 3. Prior studies of carbon isotope discrimination by tobacco showed that Rubisco fractionation (*b*) was independent of variation in mesophyll conductance, g_m, and similar between the wild-type

Table 2. *Gas exchange and biochemical properties of wild-type tobacco and transplastomic mutants tob(Rr), tob(L335V), tob(bid), and tob(flo)*

Gas exchange and carbon isotope discrimination were measured at ambient CO_2 ~380 μbar, O_2 19 mbar, irradiance 1500 μmol m^{-2} s^{-1}, and leaf temperature 25 °C. Other measurements were made on leaf material harvested from the same leaves after gas exchange measurements. ND, not determined.

Parameter	**Set 1**			**Set 2**		
	tob(Wt) (*n*=4)	**tob(Rr) (*n*=4)**	**tob(L335V) (*n*=7)**	**tob(Wt) (*n*=4)**	**tob(bid) (*n*=3)**	**tob(flo) (*n*=3)**
CO_2-assimilation rate, A (μmol CO_2 m^{-2} s^{-1})	26.0±0.8	6.6±0.2	7.1±0.3	30.2±0.9	13.4±1.9	17.0±0.4
Stomatal conductance (mol m^{-2} s^{-1})	0.57±0.08	0.57±0.04	0.31±0.04	0.64±0.06	0.52±0.07	0.74±0.07
Ratio of intercellular to ambient CO_2, C_i/C_a	0.77±0.03	0.93±0.01	0.86±0.02	0.74±0.03	0.86±0.01	0.86±0.01
Dark respiration, R_d(μmol CO_2 m^{-2} s^{-1})	1.4±0.14	0.81±0.1	1.24±0.14	1.8±0.3	1.3±0.05	1.9±0.3
Mesophyll conductance, g_m (mol m^{-2} s^{-1} bar^{-1})	0.29±0.02	ND	ND	0.46±0.07	ND	ND
Rubisco sites (μmol CO_2 m^{-2})	23.1±1.5	28.2±1.2	32.2±1.8	24.7±0.7	7.9±0.7	10.9±0.3
Maximum Rubisco activity, V_{cmax} (μmol CO_2 m^{-2} s^{-1})[a]	134±6	112±2	23.8±1	116±6	43±7	44±2
Catalytic turnover of Rubisco *in vivo*, k_{cat} (s^{-1})[b]	5.9±0.3	4.1±0.1	0.75±0.03	4.7±0.2	5.4±0.2	4.1±0.3
Soluble protein (g m^{-2})	6.7±0.4	6.1±0.2	6.7±0.0.2	7.4±0.1	7.0±0.2	6.6±0.0.2
Leaf dry mass per unit leaf area (g m^{-2})	18.2±1.5	19.2±1.4	22.8±2.3	23.1±1.0	22.6±1.2	25.5±1.8

[a] Maximum Rubisco activity, V_{cmax}, was estimated from measurements of CO_2 response curves using kinetic parameter values given in the legend of Fig. 1.

[b] k_{cat} was calculated from the ratio of V_{cmax} and Rubisco site content measured on individual leaves.

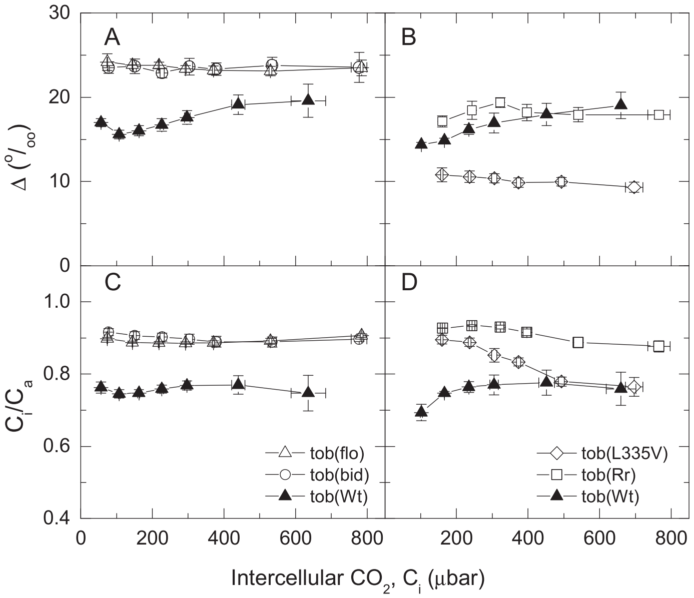

Fig. 2. Carbon isotope discrimination measured concurrently with gas exchange (A and B) and the ratio of intercellular to ambient CO_2, C_i/C_a (C and D) in tobacco wild type [tob(Wt)] and transplastomic mutants. Transplastomic mutants and gas exchange details are as described for Fig. 1.

and anti-*Rbc*S plants which yielded an estimated value of b=29‰ (Evans *et al.*, 1994). Based on these observations, the current study assumed a value for b=29‰ for wild-type tobacco to estimate g_m and then calculated b-values for Rubisco from the four tobacco mutant genotypes using equation 5 by assuming the same g_m value to that measured in wild-type leaves of comparable physiological age and development (Table 3). This assumption is examined in Fig. 4, which shows that estimated b-values are relatively insensitive to changes in g_m until it is reduced below 50% of the assumed value, where b increases. If g_m in the transplastomic lines was 25% less than in wild-type leaves, estimated b-values would increase slightly to 24, 14.3, 28.6, and 29.6‰ for tob(Rr), tob(L335V), tob(bid), and tob(flo), respectively, which is within the margin of error for the values given in Table 3.

Respiratory and photorespiratory fractionations were calculated using equations 6 and 7 (Table 3). Although CO_2-assimilation rates were lower in the four mutant tobacco genotypes (Fig. 1), the respiration rates were similar (Table 2). Consequently, the values of respiratory fractionation (Δ_e) are slightly greater for the mutants compared to tob(Wt). Photorespiratory fractionation (Δ_f) was greater in both tob(Rr) and tob(L335V) because these Rubiscos have lower $S_{c/o}$ values which increases flux through photorespiration compared to tob(wt) (Table 3). By contrast, Δ_f was similar in tob(Wt), tob(bid), and tob(flo) because of their similar Rubisco $S_{c/o}$ values (Table 3). Together, Δ_e and Δ_f are expected to account for 10–18% of the carbon isotope discrimination signal in tob(Rr) and tob(L335V) compared to 6% for tob(bid) and tob(flo).

The measured Δ values are shown with respect to C_i/C_a (Fig. 3). Theoretical lines are shown which assume infinite mesophyll conductance and ignore the influence of Δ_e and Δ_f. Taking the Δ_e and Δ_f fractionations and mesophyll conductance into account, this study found that estimates of b for tob(Rr) and tob(L335V) were significantly less than the 29‰ assumed for tob(wt) (Table 3). In contrast, there was no significant difference in the b-values of tob(Wt), tob(bid), and tob(flo).

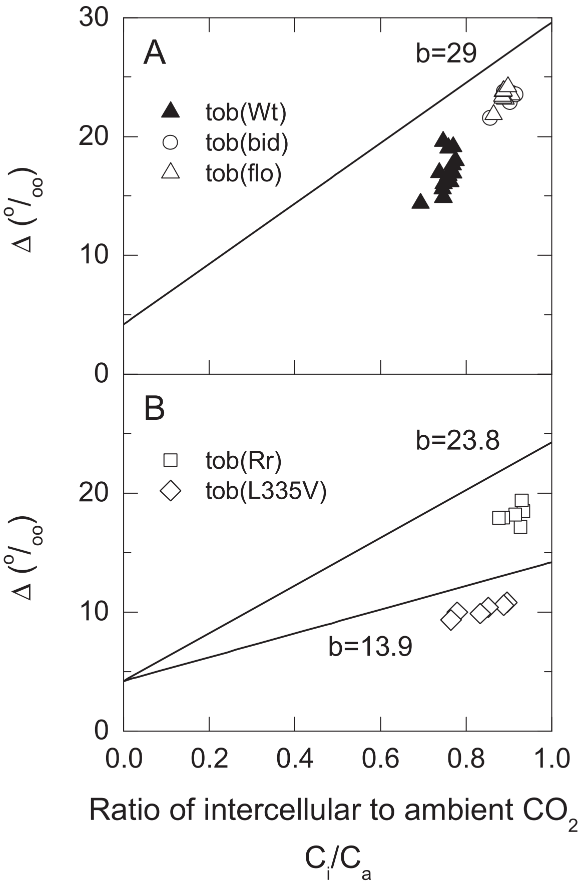

Fig. 3. Carbon isotope discrimination, Δ, as a function of the ratio of intercellular to ambient CO_2 partial pressure for tob(Wt), tob(bid), tob(flo), tob(Rr), and tob(L335V). Lines show theoretical relationships between Δ and C_i/C_a with different Rubisco discrimination factors (b) which assume an infinite g_m and no respiratory fractionations, but include the ternary correction with t=0.01 ($\Delta = 4.2 + (1.02 * b - 4.2)C_i/C_a$). Transplastomic mutants are as described for Fig. 1.

Discussion

Tobacco is established as a model species for investigations into photosynthetic metabolism as it is readily transformable via nuclear and transplastomic techniques (Rodermel *et al.*, 1988; Quick *et al.*, 1991; Hudson *et al.*, 1992; Whitney *et al.*, 1999; Maliga, 2002). This study group have extensively characterized gas exchange and carbon isotope discrimination properties in this species (Evans *et al.*, 1986, 1994; Yamori *et al.*, 2010; Tazoe *et al.*, 2011; Evans and von Caemmerer, 2013). While knowing the Rubisco discrimination factor (b) is pivotal for fully understanding plant carbon metabolism and the impact of photosynthesis on atmospheric carbon isotope signatures (Suits *et al.*, 2005; Tcherkez *et al.*, 2011), little is known about variation in b as it is difficult to measure using existing *in vitro* methods (McNevin *et al.*, 2006, 2007). Tuneable diode laser absorption spectroscopy allows rapid measurements of Δ to be made concurrently with photosynthetic gas exchange. The present study used this technique to estimate b *in vivo* in a number of transplastomic tobacco genotypes. While the technique is rapid, it relies on understanding the contribution that CO_2 diffusion and respiratory metabolism have on photosynthetic carbon isotope discrimination (equations 2 to 7). The impact of respiratory and photorespiratory fractionation was minimized by making measurements under high light and low pO_2 (Table 3). Differences in $\delta^{13}C$ values of the source and measuring CO_2 also influence Δ_e, but on average did not vary with genotype.

CO_2 diffusion has the greatest impact on the interpretation. Lower CO_2-assimilation rates in transplastomic tobacco genotypes compared to wild type were not accompanied by proportional reductions in stomatal conductance and this led to greater ratios of intercellular to ambient CO_2 (C_i/C_a) that increased discrimination (Figs 2 and 3). Similarly, lower CO_2-assimilation rates reduced the draw down in pCO_2 from

Table 3. *Leaf carbon isotope discrimination and Rubisco discrimination (*b*) as well as carbon isotope discrimination associated with respiration (Δ_e, equation 6) and photorespiration (Δ_f, equation 7) in wild-type tobacco and transplastomic mutants tob(Rr), tob(L335V), tob(bid), and tob(flo)*

Gas exchange and carbon isotope discrimination were measured at ambient CO_2 ~380 μbar, O_2 19 mbar, irradiance 1500 μmol m^{-2} s^{-1}, and leaf temperature 25 °C. To calculate Δ_f, a value for Γ_* of 4.7 μbar was used for tob(Wt), tob(bid), and tob(flo), 14.0 μbar for tob(L335V), and 31.4 μbar for tob(Rr).

Parameter	**Set 1**			**Set 2**		
	tob(Wt) (*n*=4)	**tob(Rr) (*n*=4)**	**tob(L335V) (*n*=7)**	**tob(Wt) (*n*=4)**	**tob(bid) (*n*=3)**	**tob(flo) (*n*=3)**
Δ (‰)	16.9±1.2	19.4±0.6	10.4±0.6	16.9±0.6	21.6±0.9	21.8±0.3
Rubisco discrimination, b (‰)[a]	29	23.8±0.7	13.9±0.7	29	27.8±0.8	28.6±0.6
Rubisco discrimination (b) *in vitro* (McNevin *et al.* 2007) (‰)[b]	28.5±0.9	23.3±2.1	12.3±1.6			
Δ_e (‰)	0.2±0.01	0.5±0.06	1.2±0.2	0.6±0.1	1.2±0.2	1.1±0.3
Δ_f (‰)	0.1±0.001	1.4±0.02	0.6±0.003	0.2±0.001	0.2±0.001	0.2±0.0.001

[a] Rubisco discrimination b, was estimated from Δ measured at ambient CO_2 of 380 μbar using equation 5 and the g_m value of the wild-type control (Table 2).
[b] Expressed here with respect to gaseous CO_2.

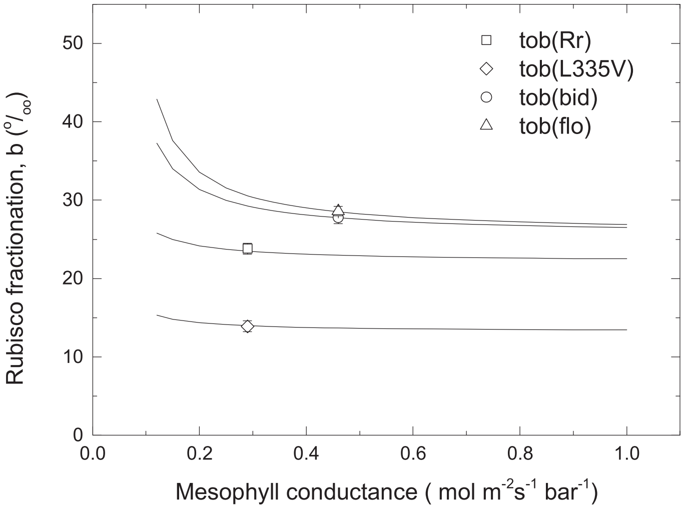

Fig. 4. Modelled dependence of estimates of Rubisco fractionation factor, *b*, on mesophyll conductance using equation 5 and values of parameters given in Tables 2 and 3. Also shown are the measured values of *b* given in Table 2. Transplastomic mutants are as described for Fig. 1.

intercellular airspace to the chloroplasts which would reduce the effect of mesophyll conductance on the isotope signal. Previous measurements of transgenic tobacco with reduced amounts of Rubisco were found to have mesophyll conductances about 20–25% less than that of wild-type leaves grown under the same conditions of irradiance, temperature, and ambient CO_2 (Evans *et al.*, 1994). When grown under elevated CO_2, as in the present case, anti-*Rbc*S plants are indistinguishable from wild type in terms of size. Consequently, under these conditions, their mesophyll conductance would be expected to be similar. Mesophyll conductance is influenced by growth irradiance between 0.2 and 0.5 mol m^2 s^{-1} bar^{-1}, having been observed for tobacco at 25 °C (Table 2; Evans *et al.*, 1994; Yamori *et al.*, 2010; Evans and von Caemmerer, 2013). It is therefore important to measure wild-type leaves of comparable physiological age and development. Galmes *et al.* (2013) reported significantly lower g_m values calculated from chlorophyll fluorescence for tob(bid) and tob(flo) compared to wild type. Their plants were grown without CO_2 supplementation, but under similar irradiance, photoperiod, temperature, and humidity to this study's growth conditions. As their values for leaf dry mass per unit area, protein and Rubisco content were similar to the values measured (Table 2), the assumption that this study could use mesophyll conductance obtained from wild-type leaves needs to be kept in mind.

The lower *b*-values calculated for Rubisco from tob(L335V) and tob(Rr) determined *in vivo* from TDL measurements match those previously determined by experimentally more demanding *in vitro* methods for L335V and *R. rubrum* Rubisco (McNevin *et al.*, 2006, 2007). For both of these enzymes, the kinetic isotopic fractionation signatures provide valuable insights into variations in the Rubisco catalytic mechanism (i.e. the carbon bond-making and -cleavage reactions; Tcherkez *et al.*, 2006; McNevin *et al.*, 2007). Transplastomic modification of other L-subunit amino acids that influence the carboxylation, decarboxylation, and hydrolysis/cleavage steps of Rubisco pose a useful approach for further dissection of the mechanistic features of Rubisco catalysis. It is also feasible that examining variation in ^{13}C fractionation among catalytically and phylogenetically diverse Rubiscos by a transplastomic approach, such as tob(bid) and tob(flo), may also be useful in identifying mechanisms that underlie the natural variation in Rubisco catalysis. The method used here for measuring carbon isotope discrimination by leaves during photosynthesis is experimentally robust and simple. However, it requires the generation of photoautotrophic transplastomic lines suitable for leaf gas exchange analysis. This has been challenging for some tobacco L-subunit mutations and some heterologous Rubisco isoforms where limitations in the folding and assembly requirements cannot be met by tobacco chloroplasts, thereby either restricting or preventing recombinant Rubisco biogenesis (Whitney *et al.*, 2001, 2011a; Parry *et al.*, 2013). As shown here for all four tobacco transplastomic genotypes, even if the introduced changes to Rubisco impair its synthesis [tob(bid) and tob(flo)] or compromise catalytic activity [tob(L335V) and tob(Rr)], these can be compensated by growth at elevated pCO_2 to enable photoautotrophic growth to maturity in soil. Gas exchange conditions can be chosen to suit the modified catalytic properties to allow concurrent assessment of carbon isotope discrimination.

Prior assessment of the hybrid Rubiscos in tob(bid) and tob(flo) showed their catalytic properties matched those of the parental *F. bidentis* and *F. floridana* Rubiscos (Whitney *et al.*, 2011b). Catalytic properties of hybrid enzymes containing tobacco S-subunits and L-subunits from either sunflower or tomato Rubisco also reflected those of the L-subunit (Sharwood *et al.*, 2008). However, the S-subunits of Rubisco have also been shown to influence catalytic properties. Ishikawa *et al.* (2011) produced hybrid Rubisco with rice L-subunits and sorghum S-subunits which increased both K_c and k_{ccat} compared to wild-type rice. The *b*-values determined for Rubisco in tob(bid) and tob(flo) matched the wild type, suggesting that, despite the C_4-like catalysis of the hybrid Rubisco in tob(bid) (i.e. increased k_{ccat} and K_c; Table 1), there is little or no variation in the carbon isotope discrimination by these C_3, C_3-C_4, and C_4 Rubiscos *in vivo*. Whelan *et al.* (1973) measured higher average *b*-values for *Sorghum bicolor* Rubisco (33.7 ± 6.6‰), although statistically this overlaps the range of *b*-values calculated here for tob(bid), tob(flo), and tob(Wt). Improving the rigor of inferring Rubisco mechanistic variations from Δ measurements clearly requires reliable measurement of this parameter for Rubisco isoforms with broader catalytic spectrums (Tcherkez *et al.*, 2006; McNevin *et al.*, 2007). As shown here, transplastomic introduction of C_4-Rubiscos into tobacco plastids provides a feasible strategy to investigate the natural diversity in *b*-values for C_4-Rubiscos that are otherwise impossible to measure by *in vivo* approaches due to the presence of their CO_2-concentrating mechanisms. Expanding this transplastomic approach to include the catalytically distinctive Rubiscos from phylogentically diverse sources (such as non-green algae and cyanobacteria) currently remain stymied by limitations in their folding and assembly in plant chloroplasts (Kanevski *et al.*, 1999; Whitney *et al.*, 2001).

Acknowledgements

The authors thank Soumi Bala for expert technical assistance with plant culture, TDL, and gas exchange measurements. This research was supported by the Australian Research Council (grants DP110104269 and FT0991407).

References

Badger MR, Andrews TJ. 1987. Co-evolution of Rubisco and CO_2 concentrating mechanisms. In: Biggins J, ed, *Progress in photosynthesis research, volume III*. Dordrecht: Martinus Nijhoff Publishers, pp 601–609.

Bernacchi CJ, Portis AR, Nakano H, von Caemmerer S, Long SP. 2002. Temperature response of mesophyll conductance. Implications for the determination of Rubisco enzyme kinetics and for limitations to photosynthesis *in vivo*. *Plant Physiology* **130,** 1992–1998.

Delgado E, Medrano H, Keys AJ, Parry MAJ. 1995. Species variation in Rubisco specificity factor. *Journal of Experimental Botany* **46,** 1775–1777.

Evans JR, Kaldenhoff R, Genty B, Terashima I. 2009. Resistances along the CO_2 diffusion pathway inside leaves. *Journal of Experimental Botany* **60,** 2235–2248.

Evans JR, Sharkey TD, Berry JA, Farquhar GD. 1986. Carbon isotope discrimination measured concurrently with gas exchange to investigate CO_2 diffusion in leaves of higher plants. *Australian Journal of Plant Physiology* **13,** 281–292.

Evans JR, von Caemmerer S. 2013. Temperature response of carbon isotope discrimination and mesophyll conductance in tobacco. *Plant, Cell and Environment* **36,** 745–756.

Evans JR, von Caemmerer S, Setchell BA, Hudson GS. 1994. The relationship between CO_2 transfer conductance and leaf anatomy in transgenic tobacco with a reduced content of Rubisco. *Australian Journal of Plant Physiology* **21,** 475–495.

Farquhar GD. 1983. On the nature of carbon isotope discrimination in C_4 species. *Australian Journal of Plant Physiology* **10,** 205–226.

Farquhar GD, Cernusak LA. 2012. Ternary effects on the gas exchange of isotopologues of carbon dioxide. *Plant, Cell and Environment* **35,** 1221–1231.

Farquhar GD, Ehleringer JR, Hubick KT. 1989a. Carbon isotope discrimination and photosynthesis. *Annual Review of Plant Physiology and Plant Molecular Biology* **40,** 503–537.

Farquhar GD, Hubick KT, Condon AG, Richards RA. 1989b. Carbon istotope fractionation and plant water use efficiency. In: Rundel PW, Ehleringer JR, Nagy KA, eds, *Stable isotopes in ecological research*. New York: Springer Verlag, pp 21–40.

Farquhar GD, von Caemmerer S, Berry JA. 1980. A biochemical-model of photosynthetic CO_2 assimilation in leaves of C_3 species. *Planta* **149,** 78–90.

Galmes J, Flexas J, Keys AJ, Cifre J, Mitchell RAC, Madgwick PJ, Haslam RP, Medrano H, Parry MAJ. 2005. Rubisco specificity factor tends to be larger in plant species from drier habitats and in species with persistent leaves. *Plant, Cell and Environment* **28,** 571–579.

Galmes J, Perdomo JA, Flexas J, Whitney SM. 2013. Photosynthetic characterization of Rubisco transplantomic lines reveals alterations on photochemistry and mesophyll conductance. *Photosynthesis Research* **115,** 153–166.

Henderson S, von Caemmerer S, Farquhar GD. 1992. Short-term measurements of carbon isotope discrimination in several C_4 species. *Australian Journal of Plant Physiology* **19,** 263–285.

Hudson GS, Evans JR, von Caemmerer S, Arvidsson YBC, Andrews TJ. 1992. Reduction of ribulose-1,5-bisphosphate carboxylase/oxygenase content by antisense RNA reduces photosynthesis in transgenic tobacco plants. *Plant Physiology* **98,** 294–302.

Ishikawa C, Hatanaka T, Misoo S, Miyake C, Fukayama H. 2011. Functional incorporation of sorghum small subunit increases the catalytic turnover rate of Rubisco in transgenic rice. *Plant Physiology* **156,** 1603–1611.

Kanevski I, Maliga P, Rhoades DF, Gutteridge S. 1999. Plastome engineering of ribulose-1,5-bisphosphate carboxylase/oxygenase in tobacco to form a sunflower large subunit and tobacco small subunit hybrid. *Plant Physiology* **119,** 133–141.

Maliga P. 2002. Engineering the plastid genome of higher plants. *Current Opinion in Plant Biology* **5,** 164–172.

McNevin DB, Badger MR, Kane HJ, Farquhar GD. 2006. Measurement of (carbon) kinetic isotope effect by Rayleigh fractionation using membrane inlet mass spectrometry for CO_2-consuming reactions. *Functional Plant Biology* **33,** 1115–1128.

McNevin DB, Badger MR, Whitney SM, von Caemmerer S, Tcherkez GGB, Farquhar GD. 2007. Differences in carbon isotope discrimination of three variants of D-ribulose-1,5-bisphosphate carboxylase/oxygenase reflect differences in their catalytic mechanisms. *Journal of Biological Chemistry* **282,** 36068–36076.

Mook WG, Koopmans M, Carter AF, Keeling CD. 1983. Seasonal, latitudinal, and secular variations in the abundance of of isotopic ratios of atmopsheric carbon dioxide. 1). Results from land stations. *Journal of Geophysical Research-Atmospheres* **88,** 10915–10933.

Mueller-Cajar O, Morell M, Whitney SM. 2007. Directed evolution of rubisco in Escherichia coli reveals a specificity-determining hydrogen bond in the form II enzyme. *Biochemistry* **46,** 14067–14074.

Parry MAJ, Andralojc PJ, Scales JC, Salvucci ME, Carmo-Silva AE, Alonso H, Whitney SM. 2013. Rubisco activity and regulation as targets for crop improvement. *Journal of Experimental Botany* **64,** 717–730.

Quick WP, Schurr U, Fichtner K, Schulze E-D, Rodermel SR, Bogorad L, Stitt M. 1991. The impact of decreased Rubisco on photosynthesis, allocation and storage in tobacco plants which have been transformed with antisense *rbcS*. *The Plant Journal* **1,** 51–58.

Rodermel SR, Abbott MS, Bogorad L. 1988. Nuclear-organelle interactions: nuclear antisense gene inhibits ribulose bisphosphate carboxylase enzyme levels in transformed tobacco plants. *Cell* **55,** 673–681.

Roeske CA, O'Leary MH. 1984. Carbon isotope effects on the enzyme-catalyzed carboxylation of ribulose bisphosphate. *Biochemistry* **23,** 6275–6284.

Ruuska SA, Andrews TJ, Badger MR, Hudson GS, Laisk A, Price GD, von Caemmerer S. 1998. The interplay between limiting processes in C_3 photosynthesis studied by rapid-response gas exchange using transgenic tobacco impaired in photosynthesis. *Australian Journal of Plant Physiology* **25,** 859–870.

Sharwood RE, von Caemmerer S, Maliga P, Whitney SM. 2008. The catalytic properties of hybrid Rubisco comprising tobacco small and sunflower large subunits mirror the kinetically equivalent source Rubiscos and can support tobacco growth. *Plant Physiology* **146,** 83–96.

Suits NS, Denning AS, Berry JA, Still CJ, Kaduk J, Miller JB, Baker IT. 2005. Simulation of carbon isotope discrimination of the terrestrial biosphere. *Global Biogeochemical Cycles* **19,** B1017.

Tazoe Y, von Caemmerer S, Badger MR, Evans JR. 2009. Light and CO_2 do not affect the mesophyll conductance to CO_2 diffusion in wheat leaves. *Journal of Experimental Botany* **60,** 2291–2301.

Tazoe Y, von Caemmerer S, Estavillo GM, Evans JR. 2011. Using tunable diode laser spectroscopy to measure carbon isotope discrimination and mesophyll conductance to CO_2 diffusion dynamically at different CO_2 concentrations. *Plant, Cell and Environment* **34,** 580–591.

Tcherkez G. 2013. Modelling the reaction mechanism of ribulose-1,5-bisphosphate carboxylase/oxygenase and consequences for kinetic parameters. *Plant, Cell and Environment* **36,** 1586–1596.

Tcherkez G, Mahe A, Hodges M. 2011. $^{12}C/^{13}C$ fractionations in plant primary metabolism. *Trends in Plant Science* **16,** 499–506.

Tcherkez GGB, Farquhar GD, Andrews TJ. 2006. Despite slow catalysis and confused substrate specificity, all ribulose bisphosphate carboxylases may be nearly perfectly optimized. *Proceedings of the National Academy of Sciences, USA* **103,** 7246–7251.

von Caemmerer S, Evans JR, Hudson GS, Andrews TJ. 1994. The kinetics of ribulose-1,5-bisphosphate carboxylase/oxygenase *in vivo* inferred from measurements of photosynthesis in leaves of transgenic tobacco. *Planta* **195,** 88–97.

von Caemmerer S, Farquhar GD. 1981. Some relationships between the biochemistry of photosynthesis and the gas exchange of leaves. *Planta* **153,** 376–387.

Walker B, Ariza LS, Kaines S, Badger MR, Cousins AB. 2013. Temperature response of *in vivo* Rubisco kinetics and mesophyll conductance in *Arabidopsis thaliana*: comparisons to *Nicotiana tabacum*. *Plant, Cell and Environment* **36,** 2108–2119.

Whelan T, Sackett WM, Benedict CR. 1973. Enzymatic fractionation of carbon isotopes by phosphoenolpyruvate carboxylase from C_4-plants. *Plant Physiology* **51,** 1051–1054.

Whitney SM, Andrews TJ. 2001. Plastome-encoded bacterial ribulose-1,5-bisphosphate carboxylase/oxygenase (RubisCO) supports photosynthesis and growth in tobacco. *Proceedings of the National Academy of Sciences, USA* **98,** 14738–14743.

Whitney SM, Andrews TJ. 2003. Photosynthesis and growth of tobacco with a substituted bacterial Rubisco mirror the properties of the introduced enzyme. *Plant Physiology* **133,** 287–294.

Whitney SM, Baldett P, Hudson GS, Andrews TJ. 2001. Form I Rubiscos from non-green algae are expressed abundantly but not assembled in tobacco chloroplasts. *The Plant Journal* **26,** 535–547.

Whitney SM, Houtz RL, Alonso H. 2011a. Advancing our understanding and capacity to engineer nature's CO_2-sequestering enzyme, Rubisco. *Plant Physiology* **155,** 27–35.

Whitney SM, Sharwood RE. 2007. Linked Rubisco subunits can assemble into functional oligomers without impeding catalytic performance. *Journal of Biological Chemistry* **282,** 3809–3818.

Whitney SM, Sharwood RE, Orr D, White SJ, Alonso H, Galmés J. 2011b. Isoleucine 309 acts as a C_4 catalytic switch that increases ribulose-1,5-bisphosphate carboxylase/oxygenase (rubisco) carboxylation rate in *Flaveria*. *Proceedings of the National Academy of Sciences, USA* **108,** 14688–14693.

Whitney SM, von Caemmerer S, Hudson GS, Andrews TJ. 1999. Directed mutation of the Rubisco large subunit of tobacco influences photorespiration and growth. *Plant Physiology* **121,** 579–588.

Yakir D, Sternberg LDL. 2000. The use of stable isotopes to study ecosystem gas exchange. *Oecologia* **123,** 297–311.

Yamori W, Evans JR, von Caemmerer S. 2010. Effects of growth and measurement light intensities on temperature dependence of CO_2 assimilation rate in tobacco leaves. *Plant, Cell and Environment* **33,** 332–343.

Yeoh H-H, Badger MR, Watson L. 1981. Variations in kinetic-properties of ribulose-1,5-bisphosphate carboxylases among plants. *Plant Physiology* **67,** 1151–1155.